

Article

Stability Analysis of the Explicit Difference Scheme for Richards Equation

Fengnan Liu ¹, Yasuhide Fukumoto ^{2,*}  and Xiaopeng Zhao ³

¹ School of Mathematical and Physical Sciences, Dalian University of Technology, Panjin 124221, China; liufengnan@dlut.edu.cn

² Institute of Mathematics for Industry, Kyushu University, 744 Motoooka, Nishi-ku, Fukuoka 819-0395, Japan

³ College of Sciences, Northeastern University, Shenyang 110819, China; zhaoxiaopeng@jiangnan.edu.cn

* Correspondence: yasuhide@imi.kyushu-u.ac.jp

Received: 6 January 2020; Accepted: 15 March 2020; Published: 18 March 2020



Abstract: A stable explicit difference scheme, which is based on forward Euler format, is proposed for the Richards equation. To avoid the degeneracy of the Richards equation, we add a perturbation to the functional coefficient of the parabolic term. In addition, we introduce an extra term in the difference scheme which is used to relax the time step restriction for improving the stability condition. With the augmented terms, we prove the stability using the induction method. Numerical experiments show the validity and the accuracy of the scheme, along with its efficiency.

Keywords: Richards equation; explicit difference scheme; stability analysis

1. Introduction

A knowledge of the way of infiltration of water into the ground is crucially important for predicting disasters, such as river floods and landslides, when heavy rain attacks. A classical mathematical model for describing the fluid motion in unsaturated zone in a porous medium is the Richards equation, a nonlinear degenerate advection-diffusion equation. Two main research directions arose recently for the Richards equation. One is to find exact solutions by finding a specific form of coefficient functions so as to make the equation completely integrable. An exact solution helps to clearly capture the physical mechanism of the phenomena and to pursue controllability [1–3]. The other research direction is to seek an approximate solution by numerical methods, for coefficient functions to match with a practical situation. Finite elements, finite difference or finite volumes methods are carried out in [4,5] and the reference therein. The above schemes commonly used fully implicit schemes based on a backward Euler format. Adaptive time stepping is studied in [6,7]. In these studies, some conservative schemes are devised and numerical tests show that they have good stability and some order accuracy, but no theoretical proof is given.

So far, we have only known one paper to prove the stability for the mixed finite element discretization of the Richards equation in [8,9]. In [8], they introduced an implicit mixed element scheme and applied the Kirchhoff transformation to deal with the degeneracy of the Richards equation. The Kirchhoff transformation could be used in the continuous inner product, but we have to take the discrete inner product in the analysis for the difference scheme, so we take a new way which is by adding a perturbation to the coefficient function of parabolic term to overcome the degeneracy.

In [8], the scheme they used is implicit, the stability condition is certainly superior to the explicit scheme. So they do not pay attention to the stability condition in the analysis for the implicit scheme. However, the explicit numerical schemes always are stable only in rigorous restriction for mesh ratio. To improve the stability condition, we introduced an extra term in the difference scheme to relax the

time step restriction for improving the stability condition. Also, the theoretical analysis for the implicit numerical schemes and the explicit difference scheme is completely different.

As we know, these early attempts are all implicit schemes based on backward Euler difference scheme and the central difference scheme, although in certain case, the implicit scheme may have to be used to avoid instability. However a strongly nonlinear algebraic system must be solved at each time level, even though these iterative methods [10,11] are used, it still needs huge calculation. Explicit scheme is a good choice to improve the computation efficiency, but the classical explicit scheme cannot be used for the Richards equation due to its degeneracy and the severe time step length restriction.

The main purpose of this work is to provide an efficient explicit numerical scheme for the Richards equation and prove the stability. The key objectives of this work are threefold: First, we add a perturbation to the coefficient function of parabolic term to overcome the degeneracy. Secondly, we introduce a stabilization term with constant coefficient in the difference scheme to relax the stability restriction on the time step. Please note that a similar technique has been used in the simulation of the Cahn–Hilliard equation [12] and the MBE models [13]. The Cahn–Hilliard equation and the MBE models are fourth-order parabolic partial differential equations, so they introduced a second-order stabilization term in the Fourier spectral scheme and finite element scheme respectively. The Richards equation is a second-order equation, so the stabilization term which is added in the explicit difference scheme is completely different. Finally, we prove the stability by induction method and perform some numerical experiments.

The organization of the paper as follows. In Section 2, an explicit difference scheme is given for the Richards equation. In Section 3, we prove the stability of such scheme. In Section 4, some numerical experiments are given. We conclude the paper in Section 5.

2. Richards Equation and the Explicit Difference Scheme

The Richards equation could be written in three equivalent forms, with either pressure head $h[L]$ or moisture content $\theta[L^3/L^3]$ as the dependent variable. We recall that the hydraulic head $h + z$ is partitioned into the pressure head $h = p/(\rho g)$ and the gravity head z , the vertical coordinate increasing upwards, with the pressure p normalized by the gravity force. Here ρ is the mass density of the fluid and g is the gravity acceleration. The constitutive relationship between $\theta = \theta(z, t)$ and $h = h(z, t)$ allows the conversion from one to another. The three forms can be identified as h -based, θ -based, and mixed:

- h -based

$$C(h) \frac{\partial h}{\partial t} - \nabla \cdot K(h) \nabla h - \frac{\partial K}{\partial z} = 0, \quad (1)$$

- θ -based

$$\frac{\partial \theta}{\partial t} - \nabla \cdot D(\theta) \nabla \theta - \frac{\partial K}{\partial z} = 0, \quad (2)$$

- mixed

$$\frac{\partial \theta}{\partial t} - \nabla \cdot K(h) \nabla h - \frac{\partial K}{\partial z} = 0, \quad (3)$$

where the real-valued functions $C(h) \equiv d\theta/dh$, $K(h)$, and $D(\theta) \equiv K(\theta)/C(\theta)$ respectively denote the specific moisture capacity function [$1/L$], the unsaturated hydraulic conductivity [L/T] and the unsaturated diffusivity [L^2/T]. The coefficient $K(h)$ describes the ease with which water can move through pore spaces, and depends on the intrinsic permeability of the material, degree of saturation, and the density and the viscosity of the fluid. The porous medium is assumed to be isotropic.

We consider the h -based form with the datum reported by Haverkamp et al. [14,15] which is used to solve an example of infiltration into soil column.

$$\theta(h) = \frac{\alpha(\theta_s - \theta_r)}{\alpha + |h|^\beta} + \theta_r, \quad K(h) = K_s \frac{A}{A + |h|^\gamma}, \quad (4)$$

where $\theta(h)$ represents the moisture content. θ_r and θ_s are initial and saturated moisture content respectively. Moreover, $C(h) = d\theta/dh$, simple calculations show that

$$C(h) = \theta'(h) = \frac{\alpha(\theta_s - \theta_r)\beta|h|^{\beta-1}}{(\alpha + |h|^\beta)^2}, \quad K'(h) = \frac{K_s A \gamma |h|^{\gamma-1}}{(A + |h|^\gamma)^2}. \tag{5}$$

For the given $\theta(h)$ and $K(h)$, we consider the following data [16].

$$\alpha = 1.611 \times 10^6, \quad \theta_s = 0.287, \quad \theta_r = 0.075, \quad \beta = 3.96, \\ K_s = 0.00944 \text{ cm/s}, \quad A = 1.175 \times 10^6, \quad \gamma = 4.74.$$

$$h(40 \text{ cm}, t) = h_{top} = -20.7 \text{ cm}, \quad h(0, t) = h_{bottom} = -61.5 \text{ cm}. \tag{6}$$

These data provide some real numbers from an example of infiltration into soil column. From the data, we can verify that there are upper bounds for $K(h)$ and $K'(h)$ easily, i.e., $K(h) \leq K < K_s, K'(h) \leq K_1$ for $h \in \mathbb{R}$. This is to be used in the stability proof.

Let $\Delta z = L/M$ be the uniform step length, where M is a positive integer. We divide the domain of time T with N segments, let $\tau = T/N, t^n = n\tau$ be the uniform time length. Then for a function $h(t, z)$, denote $H_i^n = h(z_i, t_n)$, where $z_i = m\Delta z, m = 0, 1, \dots, M$, and $\bar{\Omega} = \{z_i | i = 0, 1, \dots, M\}, t_n = n\tau, n = 0, 1, \dots, N$. Let $\lambda = \tau/\Delta z^2$ be the mesh ratios.

Define the following difference operators

$$\delta_t H_i^n = \frac{H_i^{n+1} - H_i^n}{\tau}, 0 \leq n \leq N - 1, \\ \nabla_h H_i^n = \frac{H_{i+1}^n - H_{i-1}^n}{2\Delta z}, \quad \Delta_h H_i^n = \frac{H_{i+1}^n - 2H_i^n + H_{i-1}^n}{\Delta z^2}, 1 \leq i \leq M - 1.$$

Now, we introduce the discrete L^2 inner product as $\langle u, v \rangle = \Delta z \{ \frac{1}{2}(u_0 v_0 + u_M v_M) + \sum_{i=1}^{M-1} u_i v_i \}$, and the corresponding discrete L^2 norm is $\|v\|_h = \langle v, v \rangle^{\frac{1}{2}}$. Moreover, the discrete H^1 seminorm $|\cdot|_{1,h}$ and the discrete maximum norm $|\cdot|_{\infty,h}$ are defined as

$$|v|_{1,h} = \left[\Delta z \sum_{i=1}^{M-1} (\nabla_h v_i)^2 \right]^{\frac{1}{2}}, \quad |v|_{\infty,h} = \sup_i |v_i|, i = 1, \dots, M.$$

A classical first-order explicit difference scheme is

$$C(H_i^n) \delta_t H_i^n - \nabla_h (K(H_i^n) \nabla_h H_i^n) - K'(H_i^n) \nabla_h H_i^n = 0. \tag{7}$$

For the degeneracy of the Richards equation, a special trick to handle the nonlinear parabolic term is devised. We add a positive constant ϵ_1 to $C(H_i^n)$ in (7) (in fact, ϵ_1 can be seen as a small positive bound of $C(H_i^n)$). Then modified first-order explicit scheme is of the form

$$C(H_i^n) \delta_t H_i^n + \epsilon_1 \delta_t H_i^n - \nabla_h (K(H_i^n) \nabla_h H_i^n) - K'(H_i^n) \nabla_h H_i^n = 0. \tag{8}$$

With the Richards equation featured by a convection dominated diffusion problems, numerical experiments show that the stability of (8) is restricted by the mesh ratio, meaning that the scheme is stable only in very tiny time step, as is expected. So we add extra diffusion terms in (8) to improve the stability condition so that relax the restriction of the time step.

$$C(H_i^n) \delta_t H_i^n + \epsilon_1 \delta_t H_i^n - \epsilon_2 (\Delta_h H_i^{n+1} - \Delta_h H_i^n) - \nabla_h (K(H_i^n) \nabla_h H_i^n) - K'(H_i^n) \nabla_h H_i^n = 0, \tag{9}$$

where ϵ_2 is a positive constant to be determined so as to improve the stability condition.

Remark 1. In [17], for the one-dimensional Richards equation, we also established a linearized semi-implicit finite difference scheme and analyzed the stability. Compared to the scheme of [17], the explicit difference scheme (9) is to avoid solving a linear algebraic equations at every time step. If we divide the domain of time with N segments, the explicit difference scheme could reduce the computational cost to $1/N$ of that. So the explicit difference scheme (9) is more concise and the speed of its numerical simulation is faster.

3. Stability Analysis

Theorem 1. The scheme (9) is stable with L_∞ discrete norm, when the time-step length satisfies $\tau < (C_\epsilon + \epsilon_1)K_s/K_1^2$, where the $C_\epsilon \geq 0$ is the lower bound of the $C(H_i^n)$.

Proof. From (4), the lower bound of the $K(H_i^n)$ is non-zero for the bounded $|h|$. Now we assume that there is a constant $k_\epsilon > 0$ such that $k_\epsilon < K(H_i^n), i = 0, 1, \dots, M$ for fixed n . Taking the inner product of (9) with $H^{n+1} - H^n$ gives

$$I_1 + I_2 + I_3 - I_4 = 0,$$

where I_1 – I_4 satisfy

$$I_1 = \langle (C(H^n) + \epsilon_1) \frac{H^{n+1} - H^n}{\tau}, H^{n+1} - H^n \rangle \geq (C_\epsilon + \frac{\epsilon_1}{\tau}) \|H^{n+1} - H^n\|^2,$$

$$I_2 = -\langle \epsilon_2(\Delta_h H^{n+1} - \Delta_h H^n), H^{n+1} - H^n \rangle = \epsilon_2 \|\nabla_h H^{n+1} - \nabla_h H^n\|^2,$$

$$\begin{aligned} I_3 &= \langle K(H^n) \nabla_h H^n, \nabla_h H^{n+1} - \nabla_h H^n \rangle \\ &= \langle K(H^n) (\nabla_h H^{n+1} - \nabla_h H^n), \nabla_h H^n - \nabla_h H^{n+1} + \nabla_h H^{n+1} \rangle \\ &\geq -K \|\nabla_h H^{n+1} - \nabla_h H^n\|^2 + \frac{K_\epsilon}{2} (\|\nabla_h H^{n+1}\|^2 - \|\nabla_h H^n\|^2), \end{aligned}$$

and

$$I_4 = \langle K'(H^n) \nabla_h H^n, H^{n+1} - H^n \rangle \leq \frac{\epsilon_1}{2\tau} \|H^{n+1} - H^n\|^2 + \frac{K_1^2 \tau}{2\epsilon_1} \|\nabla_h H^n\|^2.$$

Summing up, we obtain

$$\begin{aligned} &(C_\epsilon + \frac{\epsilon_1}{2\tau}) \|H^{n+1} - H^n\|^2 + (\epsilon_2 - K) \|\nabla_h H^{n+1} - \nabla_h H^n\|^2 \\ &+ \frac{K_s}{2} (\|\nabla_h H^{n+1}\|^2 - \|\nabla_h H^n\|^2) \leq \frac{K_1^2 \tau}{2\epsilon_1} \|\nabla_h H^n\|^2, \end{aligned}$$

for $\epsilon_2 \geq K$. Simple calculation shows that

$$\|\nabla_h H^{n+1}\|^2 \leq (1 + \frac{K_1^2 \tau}{\epsilon_1 K_s}) \|\nabla_h H^n\|^2, \tag{10}$$

which implies that there exists a positive constant c_1 , being independent of Δz and τ , such that $\|\nabla_h H^{n+1}\|^2 \leq c_1$.

We are now prepared to prove the stability with respect to the discrete L^2 norm. Taking the inner product of (9) with H^{n+1} , we have

$$E_1 + E_2 + F_1 \leq E_3 + F_2 + E_5,$$

where

$$E_1 = \langle (C(H^n) + \epsilon_1) \frac{H^{n+1} - H^n}{\tau}, H^{n+1} \rangle \geq \frac{C_\epsilon + \epsilon_1}{2\tau} (\|H^{n+1}\|^2 - \|H^n\|^2),$$

$$E_2 = -\langle \epsilon_2 \Delta_h H^{n+1}, H^{n+1} \rangle = \epsilon_2 \|\nabla_h H^{n+1}\|^2,$$

$$\begin{aligned}
 E_3 &= -\langle \epsilon_2 \Delta_h H^n, H^{n+1} \rangle \leq \frac{\epsilon_2}{2} (\|\nabla_h H^{n+1}\|^2 + \|\nabla_h H^n\|^2), \\
 E_4 &= \langle K(H^n) \nabla_h H^n, \nabla_h H^{n+1} \rangle = \langle K(H^n) \nabla_h H^n, \nabla_h H^{n+1} - \nabla_h H^n + \nabla_h H^n \rangle, \\
 &= \underbrace{\langle K(H^n) \nabla_h H^n, \nabla_h H^n \rangle}_{F_1} + \underbrace{\langle K(H^n) \nabla_h H^n, \nabla_h H^{n+1} - \nabla_h H^n \rangle}_{F_2}, \\
 E_5 &= \langle K'(H^n) \nabla_h H^n, H^{n+1} \rangle \leq \frac{K_\epsilon}{2} \|\nabla_h H^n\|^2 + \frac{K_1^2}{2K_\epsilon} \|H^{n+1}\|^2.
 \end{aligned}$$

Applying Young’s inequality, we obtain

$$F_1 \geq K_\epsilon \|\nabla_h H^n\|^2, \quad F_2 \leq \frac{K}{2} (\|\nabla_h H^{n+1}\|^2 - \|\nabla_h H^n\|^2).$$

Eventually, we obtain

$$\left(\frac{C_\epsilon + \epsilon_1}{2\tau} - \frac{K_1^2}{2K_\epsilon}\right) \|H^{n+1}\|^2 + \left(\frac{K_\epsilon}{2} - \frac{\epsilon_2}{2} + \frac{K}{2}\right) \|\nabla_h H^n\|^2 + \left(\frac{\epsilon_2}{2} - \frac{K}{2}\right) \|\nabla_h H^{n+1}\|^2 \leq \frac{C_\epsilon + \epsilon_1}{2\tau} \|H^n\|^2.$$

We conclude that for $\tau < (C_\epsilon + \epsilon_1)K_s/K_1^2$, there is a positive constant c_2 which is independent of Δz and τ such that

$$\|H^{n+1}\|^2 \leq c_2. \tag{11}$$

Combining the above two results (11) and (10), using Sobolev’s embedding inequality, we can get $|H^{n+1}|_{\infty,h}$ is bounded when $n \rightarrow \infty$. It implies the inductive hypothesis holds, completing the proof. □

Similar estimation techniques were used in other useful applications [18].

Remark 2. We exploit the constant ϵ_2 to improve the stability. If $\epsilon_2 > K$, the scheme (9) is stable. Please note that $K < K_s$ and $K_s = 0.00944\text{cm/s}$ makes it possible to take ϵ_2 sufficiently small in case of excessive errors.

Remark 3. To make sure the numerical scheme (9) is convergent, the time step should be chosen to satisfy $\tau < (C_\epsilon + \epsilon_1)K_s/K_1^2$. If $C_\epsilon = 0$, we have to take a non-zero perturbation ϵ_1 to ensure the stability of the scheme. Because of $C_\epsilon > 0$, we are allowed to take $\epsilon_1 = 0$ in numerical experiments.

4. Numerical Experiments

In this section, we illustrate the numerical stability by a numerical experiment of the infiltration process based on a generalized h -based Richards equation. Since it is difficult to obtain the exact solution of this model, to verify the theoretical results, we take the following non-homogeneous model,

$$\begin{cases} C(h) \frac{\partial h}{\partial t} - \nabla \cdot (K(h) \nabla h) - \frac{\partial K}{\partial z} = g(z, t), \\ h(z, 0) = -1.02z - 20.7, \end{cases}$$

where the boundary conditions remain unchanged as (6). If we suppose an exact solution $h = -1.02 - 20.7 + t(z - 40)/(4T)$, a simple calculation shows that

$$g(z, t) = \frac{5808800331328389z(z - 40) \left(\frac{51z}{50} - \frac{tz(z-40)}{4T} + \frac{207}{10} \right)^{74/25}}{17179869184T \left[\left(\frac{51z}{50} - \frac{tz(z-40)}{4T} + \frac{207}{10} \right)^{99/25} + 1611000 \right]^2} - \frac{5546t}{\left(\frac{51z}{50} - \frac{tz(z-40)}{4T} + \frac{207}{10} \right)^{237/50} + 1175000} - \frac{3613000706430075 \left(\frac{t(z-20)}{2T} - \frac{51}{50} \right) \left(\frac{51z}{50} - \frac{tz(z-40)}{4T} + \frac{207}{10} \right)^{187/50}}{68719476736 \left[\left(\frac{51z}{50} - \frac{tz(z-40)}{4T} + \frac{207}{10} \right)^{237/50} + 1175000 \right]^2}.$$

By using the scheme (9), we show, in Figure 1, the variation trend of the pressure head with depth for the time interval from 10 s to 360 s, with the choice of $\epsilon_1 = 0$ and $\epsilon_2 = 0$.

In [14], the authors used an implicit numerical scheme, and took a large time step, for instance, 10 s, 30 s and 120 s, to save the computational workload. In this paper, we take the time step as small as 10^{-3} s. Correspondingly the space steps that they used are much larger than ours. The different scheme and the large grid gap may bring some but tolerable discrepancy.

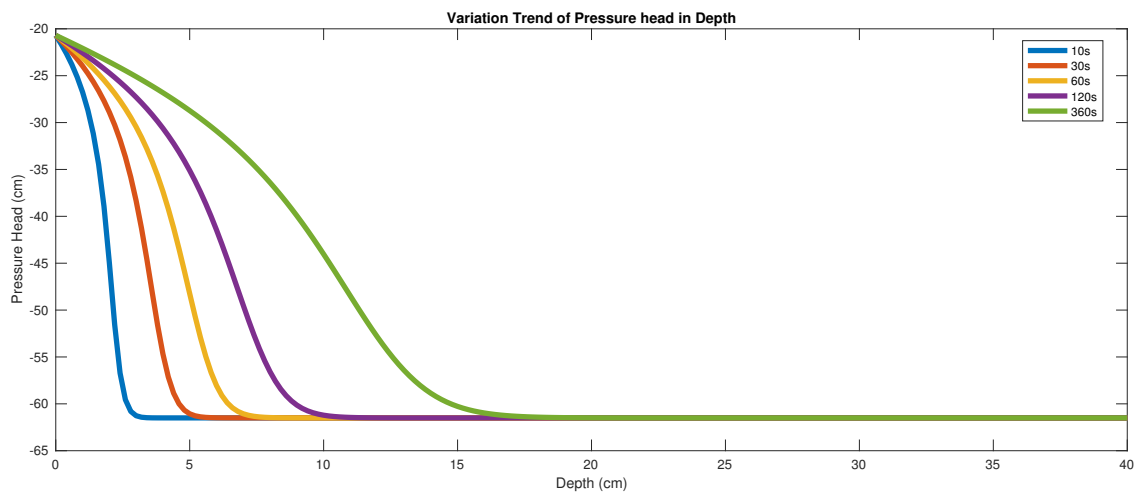


Figure 1. Variation of the pressure head with depth.

We take $T = 100$ s and $M = 200$ to test the stability of the scheme with different time steps and different choices of ϵ_2 . The results are listed in Table 1. It is evident that the improvement in the stability by use of the extra terms is significant. Moreover, in Table 2, we set $\epsilon_1 = 0, \epsilon_2 = 0, M = 200$ and $T = 1$ s, and confirm that the expected order of convergence is obtained.

Table 1. Stability comparison with different ϵ_2 and τ .

Accuracy τ	$\tau = 0.4$	$\tau = 0.2$	$\tau = 0.1$	$\tau = 0.05$	$\tau = 0.025$	$\tau = 0.0125$
$\epsilon_2 = 0$	Unstable	Unstable	Unstable	Unstable	5.60×10^{-4}	3.26×10^{-5}
$\epsilon_2 = 0.0001$	Unstable	Unstable	Unstable	Unstable	1.38×10^{-4}	3.75×10^{-5}
$\epsilon_2 = 0.0005$	Unstable	1.88×10^{-1}	5.47×10^{-2}	5.00×10^{-3}	3.78×10^{-4}	1.90×10^{-4}
$\epsilon_2 = 0.001$	9.10×10^{-2}	1.44×10^{-2}	4.00×10^{-3}	1.50×10^{-3}	7.54×10^{-4}	3.79×10^{-4}

Table 2. Accuracy.

N	1000	2000	4000	8000	16,000
$ h - H _{\infty, h}$	1.90×10^{-3}	9.65×10^{-4}	4.82×10^{-4}	2.41×10^{-4}	1.21×10^{-4}
Ratio	Non	0.98	1.00	1.00	0.99

Figure 2 shows the linear relationship between ϵ_1 and errors.

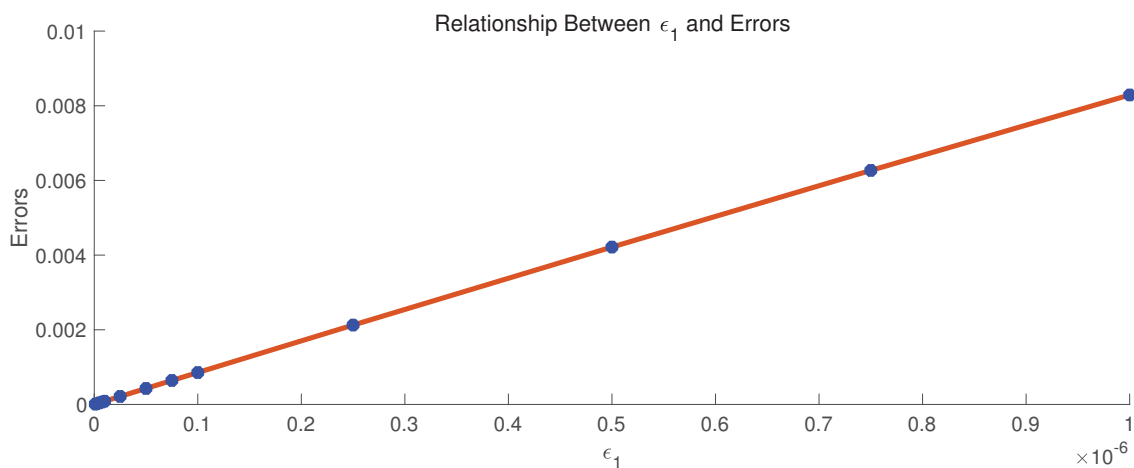


Figure 2. Relationship between ϵ_1 and errors.

5. Conclusions

In this work, a stable explicit scheme for the Richards equation was developed and analyzed. We proposed techniques to avoid the degeneracy of the Richards equation and improve the stability condition of the finite difference scheme. A numerical example is provided to verify our theoretical analysis. Demonstration of the numerical stability over a long time, along with the error estimate as shown by Figure 2, is indicative of the physical stability of a typical solution of the Richards equation; infinitesimal perturbations to the solution do not grow. A rigorous mathematical analysis of the stability of the traveling-wave solution and its relevance to the numerical stability call for an independent investigation.

Compared to implicit numerical schemes and linearized numerical schemes, stable explicit numerical schemes improve the calculation efficiency. This paper is a first step toward the explicit difference schemes for the Richards equation, we only analysis the stability of such a scheme. It is our ongoing work to extend other high order accuracy explicit difference schemes and estimate the errors.

Author Contributions: Conceptualization, Y.F., F.L. and X.Z.; Methodology, F.L. and X.Z.; Calculation, F.L.; Validation, X.Z. and Y.F.; Formal Analysis, F.L.; Data Curation, F.L.; Writing—Original Draft Preparation, F.L.; Writing—Review Editing, Y.F., F.L. and X.Z. All authors have read and agreed to the published version of the manuscript.

Funding: F.L. was supported by Fundamental Research Funds for Central Universities (no. DUT19RC(4)038), Y.F. was supported by a Grant-in-Aid for Scientific Research from the Japan Society for the Promotion of Science (grant no.19K03672), and X.Z. was supported by China Postdoctoral Science Foundation (no. 2015M581689).

Conflicts of Interest: The authors declare no conflict of interest.

References

- Broadbridge, P.; Daly, E.; Goard, J. Exact Solutions of the Richards Equation With Nonlinear Plant-Root Extraction. *Water Resour. Res.* **2017**, *53*, 9679–9691. [[CrossRef](#)]
- Broadbridge, P.; Edwards, M.; Kearton, J. Closed-form solutions for unsaturated flow under variable flux boundary conditions. *Adv. Water Res.* **1996**, *19*, 207–213. [[CrossRef](#)]

3. Broadbridge, P.; Triadis, D.; Hill, J.M. Infiltration from supply at constant water content: an integrable model. *J. Eng. Math.* **2009**, *64*, 193–206. [[CrossRef](#)]
4. Kumar, C. A numerical simulation model for one-dimensional infiltration. *ISH J. Hydraul. Eng.* **1998**, *4*, 5–15. [[CrossRef](#)]
5. Lopez, F.; Vacca, G. Spectral properties and conservation laws in mimetic finite difference methods for PDEs. *J. Comput. Appl. Math.* **2016**, *292*, 760–784. [[CrossRef](#)]
6. Kavetski, D.; Binning, P.; Sloan, S.W. Adaptive time stepping and error control in a mass conservative numerical solution of the mixed form of Richards equation. *Adv. Water Res.* **2001**, *24*, 595–605. [[CrossRef](#)]
7. Williams, G.A.; Miller, C.T. An evaluation of temporally adaptive transformation approaches for solving Richards equation. *Adv. Water Res.* **1999**, *22*, 831–840. [[CrossRef](#)]
8. Radu, F.; Pop, I.S.; Knabner, P. Order of convergence estimates for an Euler implicit, mixed finite element discretization of Richards equation. *SIAM J. Numer. Anal.* **2004**, *42*, 1452–1478. [[CrossRef](#)]
9. Both, J.W.; Kumar, K.; Nordbotten, J.M.; Pop, I.S.; Radu, F.A. Iterative Linearisation Schemes for Doubly Degenerate Parabolic Equations. In *Numerical Mathematics and Advanced Applications*; Springer: Cham, Switzerland, 2017; Volume 126.
10. Kuraz, M.; Mayer, P.; Pech, P. Solving the nonlinear Richards equation model with adaptive domain decomposition. *J. Comput. Appl. Math.* **2014**, *270*, 2–11. [[CrossRef](#)]
11. List, F.; Radu, F.A. A study on iterative methods for solving Richards' equation. *Comput. Geosci.* **2016**, *20*, 341–353. [[CrossRef](#)]
12. Zhu, J.; Chen, L.-Q.; Shen, J.; Tikare, V. Coarsening kinetics from a variable-mobility Cahn-Hilliard equation: Application of a semi-implicit Fourier spectral method. *Phys. Rev. E* **1999**, *60*, 3564–3572. [[CrossRef](#)] [[PubMed](#)]
13. Xu, C.; Tang, T. Stability analysis of large time-stepping methods for epitaxial growth models. *SIAM J. Numer. Anal.* **2006**, *44*, 1759–1779. [[CrossRef](#)]
14. Haverkamp, R.; Vauclin, M. A note on estimating finite difference interblock hydraulic conductivity values for transient unsaturated flow problems. *Water Resour. Res.* **1979**, *15*, 181–187. [[CrossRef](#)]
15. Pop, I.S.; Radu, F.; Knabner, P. Mixed finite elements for the Richards' equation: linearization procedure. *J. Comput. Appl. Math.* **2004**, *168*, 365–373. [[CrossRef](#)]
16. Celia, M.A.; Bouloutas, E.T. A general mass-conservative numerical solution for the unsaturated flow equation. *Water Resour. Res.* **1990**, *26*, 1483–1496. [[CrossRef](#)]
17. Liu, F.; Fukumoto, Y.; Zhao, X. A linearized finite difference scheme for the Richards equation under variable-flux boundary conditions. *J. Sci. Comput.* **2020**, in press. [[CrossRef](#)]
18. Shang, Y. Fixed-time group consensus for multi-agent systems with non-linear dynamics and uncertainties. *IET control Theory Appl.* **2018**, *12*, 395–404. [[CrossRef](#)]



© 2020 by the authors. Licensee MDPI, Basel, Switzerland. This article is an open access article distributed under the terms and conditions of the Creative Commons Attribution (CC BY) license (<http://creativecommons.org/licenses/by/4.0/>).